Measurement of oscillator strengths of the principal series of calcium

Ishaq Ahmad and M. A. Baig*
Atomic and Molecular Physics Laboratory, Department of Physics, Quaid-i-Azam University, Islamabad, Pakistan and Physikalisches Institut der Universität Bonn, Nussallee 12, D-53115 Bonn, Germany

Josef Hormes
Physikalisches Institut der Universität Bonn, Nussallee 12, D-53115 Bonn, Germany
(Received 18 October 1993)

Measurements of oscillator strengths for the principal series of calcium $4s^2\,{}^1S_0 \rightarrow 4snp\,{}^1P_1$ ($11 \leq n \leq 25$) are reported. The data were acquired using the magneto-optical spectroscopic technique, utilizing the linearly polarized light emitted by the 2.5-GeV electron accelerator, a 7-T superconducting magnet, and a 3-m-high dispersion spectrograph with photographic detection. A quantum-defect plot of the density of the oscillator strengths of discrete transitions yields the photoionization cross section at threshold as 2.04 ± 0.20 Mb, in agreement with earlier measurements.

PACS number(s): 32.30.Jc, 32.60.+i, 32.70.Cs, 32.70.Fw

I. INTRODUCTION

Magneto-optical rotation absorption spectroscopy is one of the well-established experimental techniques to determine the oscillator strengths of atomic and molecular transitions. In this method, the rotation of the plane of polarization of linearly polarized light is probed when light passes through an absorption column in the presence of the magnetic field. When the atomic vapor is magnetized and is viewed in the direction of the magnetic field, each absorption line splits into a right circularly polarized σ^+ and a left circularly polarized σ^- component (Zeeman effect). These components correspond to transitions $\Delta m = \pm 1$, respectively, where Δm is the difference in the magnetic quantum number between the upper and the lower energy levels. Since the linearly polarized light is considered to be the result of opposite circular motions of the same frequency, it can be resolved into a right circularly polarized and a left circularly polarized component. As the refractive index is inversely proportional to the propagating velocity of the motion, the right circularly polarized radiation travels slower outside and faster inside the region between σ^- and σ^+ components. Because of this difference in velocity, the plane of the resulting light is at an angle to that of the incident light. Thus the rotation of the plane of polarization arises from the difference in refractive indices which is directly proportional to Nfl, where N is the number density of the absorbing atoms, l is the length of the absorption column, and f is the oscillator strength.

The determination of the f values from the far wings of the resonance atomic transitions using the magneto-optical rotation technique has been discussed by Mitchell and Zemansky [1] who also summarize the early work. Huber and Sandeman [2] described the linear and nonlinear optical techniques to measure oscillator strengths and transition probabilities. The method of resonant magneto-optical rotation by use of a narrow bandwidth tunable dye laser was described by; Gawlik *et al.* [3]. Garton *et al.* [4] and Alexa *et al.* [5] reported the application of the magneto-optical rotation in determining the relative f values of the Rydberg series in strontium using synchrotron radiation as the light source, a 4-T superconducting magnet, and a high-resolution spectrograph. Recently, Connerade *et al.* [6,7] have reported the measurements of f values of higher members of the principal series in SrI and BaI using synchronized pulsed magnetic fields in conjunction with a pulsed laser.

The measurements of oscillator strengths for the calcium Rydberg series have been reported [8,9] using the "hook" method. In the *hook* method, the values of Nf are derived from measurements of the refractive index, by an interference technique, close to an absorption line in the range of anomalous dispersion. The distances between the *hook* peaks situated on either side of the spectral line are measured and the Nf values are extracted with a high accuracy. Smith and Liszt [10] measured the oscillator strength of the $4s$-$4p\,{}^1P_1$ resonance transition. Similar measurements were performed by Parkinson, Reeves, and Tomkins [11], who determined the oscillator strengths for the principal series, $4snp\,{}^1P_1$ ($4 \leq n \leq 16$), the doubly excited level $3d4s\,{}^1P_1$, and the intercombination $4s4p\,{}^3P_1$ line. The absolute scale was set by reference to the density-independent measurements of the f values for the resonance line [10]. Smith and Raggett [12] reported the relative oscillator strengths of 37 lines of calcium, to an accuracy of 5%, using the absorption method. Subsequently, Wynne and Beigang [13] measured the relative oscillator strengths of the $4snp\,{}^1P_1$ ($10 \leq n \leq 13$) to an accuracy of 2% using the phase-matched nonlinear optical technique. The relative f values for a few

*Present address: Department of Physics, University of Virginia, Charlottesville, VA 22901.

members of the sharp and diffuse series, originating from the $4s4p\ ^3P_{012}$ metastable level, have been measured [14] using the hook method.

The photoionization cross section of calcium above the ionization threshold has been extensively studied [15–18] using conventional light sources. However, synchrotron radiation has also been utilized for such studies [19,20]. Karamatskos *et al.* [19] measured the photoionization spectrum of calcium in the autoionizing Rydberg series using synchrotron radiation and the atomic-beam technique, whereas, Griesmann *et al.* [20] measured the cross section of the doubly excited resonances using synchrotron radiation and a "hot-wire" thermionic diode ion detector. Griesmann *et al.* [20] calibrated their data by using the absolute measurements of the absorption cross section at threshold, $\sigma=3.4\pm0.7$ Mb, which they obtained by the multichannel quantum-defect theory extrapolation of the discrete data [8,11] and the peak of the broad $3d5p\ ^1P_1$ line at 1886 Å, $\sigma=52\pm2$ Mb (McIlrath and Sandeman [18]).

In continuation of our work on the magneto-optical rotation spectroscopy using synchrotron radiation, extensive investigations have been carried out on the spectra of magnesium, strontium, silver, and lead [21–23]. The present paper deals with measurements and interpretation of the relative f values of the principal series of CaI $2snp\ ^1P_1$ $(11\leq n\leq 25)$. We believe that accurate measurements of the oscillator strengths in calcium extending to high principal quantum numbers have not been previously reported.

II. EXPERIMENTAL PROCEDURE

The spectra were recorded using a 3-m off-plane Eagle mounting spectrograph equipped with a 6000 lines/mm holographic grating and synchrotron radiation emitted by the 2.5-GeV electron accelerator at the Bonn University as the background source of continuum. The reciprocal dispersion of the spectrograph was 0.51 Å/mm at 2000 Å [24,25]. An absorption column of about 50 cm length was obtained by using a simple wire-wound furnace 150 cm in length, with an inner diameter of 32 mm and a wall thickness of 2 mm heated by the heating element. The heating zone of the furnace was limited to only 50 cm because the superconducting solenoid produces a homogeneous magnetic field in a 60-cm-long column along its central axis. The outer surface of the furnace was covered by a water jacket to maintain it at a lower temperature. The whole furnace assembly was laid into the warm bore of the 6-T superconducting solenoids (run at 5.7 T during the experiment) and the temperature of the furnace was maintained to about ±10%. About 1 to 2 Torr of helium was admitted into the furnace as a buffer gas. This helped to contain the calcium vapor in the homogeneous zone of the magnetic field. It also helped to protect the CaF_2 window, which shielded the synchrotron vacuum.

The spectra were photographed on the Kodak short-wavelength-region plates with exposure times ranging between 6 and 8 min. The copper emission lines [26] emitted by a hollow cathode were used as the wavelength standards. The spectra recorded on the photographic plates were digitized with a computer-controlled microdensitometer at the Astronomy Institute, Bonn University. The light intensity transmitted by the photographic plate was measured in steps of 5 μm. A spectral range of about 120 Å is covered on a 20-cm-long photographic plate. The digitized spectrum therefore consists of 40 000 data points. For further analysis the desired section of the line profiles was extracted from the complete digitized spectrum.

III. DETERMINATION OF THE OSCILLATOR STRENGTH

The analysis of the observed magneto-optical spectra is described as a Vernier method by considering the full profile of the absorption lines and including contributions due to birefringence and dichroism. We represent the synchrotron radiation as elliptically polarized, in contrast to the Connerade [27], Connerade, Stavrakas, and Baig [28] assumption that it is perfectly plane polarized having right (+) and left (−) circularly polarized components of the same magnitude. This conclusion is based on our experimental results. Since the synchrotron radiation is plane polarized in the plane of the electron orbit and circularly polarized above or below the orbital plane, the intensity of the polarized component depends on the part of the synchrotron radiation being focused on the entrance slit of the spectrograph. The experimental arrangements were such that the spectrograph entrance slit was slightly out of the plane of the electron orbit, therefore, accepting the elliptically polarized component of the synchrotron light.

The propagation of the synchrotron light through an active medium is therefore represented by resolving the electric field into the right (+) and left (−) circularly polarized components of frequency ω along the z axis as

$$E_{\pm}(z,t)=(1+a)E_0\exp[i\omega(t-\tilde{n}_{\pm}z/c)](\mathbf{i}\pm i\mathbf{j}) , \tag{1}$$

where $\mathbf{i}$ and $\mathbf{j}$ are the unit vectors along the x and y axes, z is the distance traveled through the active medium, i.e., the length of the absorption column l, a is the asymmetry parameter (for $a=0$ one obtains the linearly polarized light), and $\tilde{n}_{\pm}$ is the complex refractive index, defined as

$$\tilde{n}_{\pm}=n_{\pm}-ik_{\pm} . \tag{2}$$

The components of the propagating light are represented as

$$\begin{aligned} E(z,t)&=E_{+}(z,t)+E_{-}(z,t)\\ &=E_x(z,t)\mathbf{i}+E_y(z,t)\mathbf{j} . \end{aligned} \tag{3}$$

Solving for the x and y components, we obtain

$$\begin{aligned} E_x(z,t)=\{&(1+a)\exp(-i\omega\tilde{n}_{+}z/c)\\ &+(1-a)\exp(-i\omega\tilde{n}_{-}z/c)\}E_0\exp(i\omega t) , \end{aligned} \tag{4}$$

$$\begin{aligned} E_y(z,t)=\{&(1+a)\exp(-i\omega\tilde{n}_{+}z/c)\\ &-(1-a)\exp(-i\omega\tilde{n}_{-}z/c)\}iE_0\exp(i\omega t) . \end{aligned} \tag{5}$$

Dividing expression (4) by expression (5), and with some mathematical manipulation, we arrive at a much simplified expression

$$\frac{E_y(z,t)}{E_x(z,t)} = i\frac{(1-\exp(2i\Phi))}{(1+\exp(2i\Phi))} = \tan(\Phi) , \tag{6}$$

where

$$\Phi = \phi - i\vartheta \tag{7}$$

is the complex magneto-optical angle that represents the two separate contributions from the Faraday rotation and the circular dichroism. The Faraday rotation, or circular birefringence,

$$\phi = (n_+ - n_-)l\omega/2c \tag{8}$$

arises because of the difference between the refractive indices n_+ and n_-, and it causes the rotation of the plane of polarization of the light about the direction of the propagation. The circular dichroism contribution

$$\vartheta = (k_+ - k_-)l\omega/2c - \tfrac{1}{2}\ln\{(1-a)/(1+a)\} \tag{9}$$

arises due to the differential absorption of σ^+ and σ^- components of the light. In our experimental arrangement the diffraction grating serves as a polarizing element; we therefore, denote the efficiency of the grating as P. The reflection of the grating is more if the electric field component of the incoming light is parallel to the grooves of the grating. The radiation from the synchrotron is polarized in the plane of the orbit of electrons say xz plane. Hence our experimental setup makes a combination of crossed polarizers for the radiation before it falls on the photographic plate. Considering the grooves of the grating to be in the y direction, E_x and E_y of the incoming radiation after reflection from the grating (transmitted through the analyzer) then become $[(1-P)/2]^{1/2}E_x$ and $[(1+P)/2]^{1/2}E_y$. Therefore, the intensity of the light after passing through the crossed polarizers is

$$I = (1-P)I_x/2 + (1+P)I_y/2 , \tag{10}$$

where

$$P = \frac{(I_y - I_x)}{(I_y + I_x)} . \tag{11}$$

Here I_x is the intensity of the light with the electric field vector in the x direction and I_y is the intensity of the light with the electric field vector in the y direction. Hence the intensity of the light finally falling on the photographic plate is given by the following expression:

$$\begin{aligned} I = {} & (I_0/4)[(1-a)\exp(-2k_- l\omega/c) \\ & + (1+a)\exp(-2k_+ l\omega/c)] \\ & + (I_0/2)[(1-a^2)P(2\sin^2\phi - 1) \\ & \times \exp(k_+ + k_-)(l\omega/c)] . \end{aligned} \tag{12}$$

On the basis of the standard dispersion theory for the singlet-singlet transition [1], $k_\pm$ and $n_\pm$ are expressed as functions of oscillator strength f, magnetic field B, and frequency detuning $(\nu - \nu_0)$ as

$$k_\pm = \frac{e^2 Nf}{2\omega m} \frac{\Gamma/4\pi}{(\nu_0 - \nu \pm \beta)^2 + (\Gamma/4\pi)^2} , \tag{13}$$

$$n_\pm - 1 = \frac{e^2 Nf}{4\pi m(\nu_0 \pm \beta)} \frac{(\nu_0 - \nu \pm \beta)}{(\nu_0 - \nu \pm \beta)^2 + (\Gamma/4\pi)^2} , \tag{14}$$

where $(\Gamma/4\pi)$ is the width of the line profile, ν_0 is the line center in the absence of the magnetic field, and $\beta = (eB/4\pi mc)$ gives the frequency shifts of the normal Zeeman components. Substituting Eqs. (13) and (14) in Eq. (12) for the transmitted intensity, we get a direct relation between the oscillator strength (i.e., the Nfl product) and the Faraday rotation angle. For the numerical calculations and the least-squares fitting, we have used a more elaborate expressions for $n_\pm$ and $k_\pm$ using Voigt line profiles, which include the combined effects of the Doppler broadening and the natural line width (cf. Dussa [23]). By fitting the experimental line profile to this theoretical formula for the transmitted intensity [Eq. (12), we have extracted the product of Nfl for all the lines recorded on one photographic plate. The relative f values are, therefore, determined more accurately for the entire Rydberg series, which was recorded on a single photographic plate under the identical experimental conditions, because N and l remain constant, whereas the f values vary among the members of the Rydberg series.

IV. RESULTS AND INTERPRETATION

The electric-dipole allowed transitions from the $4s^2\,{}^1S_0$ ground state of calcium are $4snp\,{}^1P_1$ $(4 \le n \le \infty)$. The resonance level $4s4p\,{}^1P_1$ lies at 4226.7 Å, whereas the intercombination line $4s4p\,{}^3P_1$, which arises due to the breakdown of the ΔS selection rule, lies at 6572.78 Å. The doubly excited states arise due to the simultaneous excitation of both the $4s$ valence electrons $4s^2{}^1S_0 \rightarrow 3dnp\,{}^1P_1$, which gives rise to a Rydberg series terminating on to the first excited state of the ion. The leading member of the doubly excited Rydberg series $3dnp\,{}^1P_1$ has been located at 2275.46 Å [29] and it lies in between the $4s6p\,{}^1P_1$ and $4s7p\,{}^1P_1$ levels of the principal series. Photoabsorption studies of the principal series [29–31] show a systematic decline in the effective quantum number at high n values. Subsequent studies of the even and the odd parity Rydberg states by multiphoton excitation [32] and multichannel quantum-defect theory analysis confirm the configuration interaction between the $4snp\,{}^1P_1$ series and the $3d4p\,{}^1P_1$ level. The lowest member of the doubly excited Rydberg series perturbs the entire principal series, whereas the higher members of the doubly excited series, which lie above the first ionization threshold, perturb the continuous spectrum and show pronounced autoionizing resonances in the $4s\varepsilon p\ J = 1$ continuum.

The perturbation in the principal series caused by the $3d4p\,{}^1P_1$ level not only induces energy shifts in the series but also disturbs the decreasing trend of the oscillator strengths and gives rise to a resonance in the discrete spectrum. According to Seaton's theorem [33], a smooth extrapolation from both the discrete and the continuum sides of the ionization threshold must match to yield the same oscillator strength density at the threshold. The intrinsic behavior of the spectral distribution of f values was interpreted by Geiger [34] using the multichannel quantum-defect theory and by Barrientos and Martin [35] using the quantum-defect orbital calculations. Geiger [34] confirmed the 2.2 multiplication factor suggested by McIlrath and Sandeman [18] to put all the ex-

isting experimental data above and below the ionization threshold on an absolute and consistent scale.

In the present work, we have determined the relative oscillator strengths (f values) of the principal series of calcium ($11 \leq n \leq 25$) using the magneto-optical rotation technique. The observed magneto-optical absorption spectrum of calcium covering the spectral region between 2020–2090 Å is presented in Fig. 1. The strong and broad line lying just above the ionization threshold corresponds to the $3s4p\ ^1P_1$ transition of MgI, which appears as an impurity in the calcium sample.

The magneto-optical rotation pattern of the $4s11p\ ^1P_1$ level of calcium is shown in Fig. 2. The normal Zeeman effect splits the $4s11p\ ^1P_1$ line into two Lorentz components labeled as σ^+ and σ^-, which appear near the center of the pattern. The magneto-optical *beats* appear symmetrically about the line center at zero magnetic field. The first minimum in the profile appears when the electric vector of the incoming light rotates by $\pi/2$ radians, the far wing region. As the frequency of the incoming radiation is tuned, the electric-field vector rotates further by π radians and a maximum occurs in the transmitted intensity, polarizer, and analyzer in phase. This rotation grows from zero to high angles as a function of photon energy, which results in maxima and minima in the signal as $\sin^2\Phi$. The observed line profile is then fitted, using Eq. (12), by a least-squares fitting routine to extract the relevant parameters.

The experimentally observed magneto-optical rotation pattern for the $4s11p\ ^1P_1$ transition and the least-squares fitted pattern are shown in Fig. 2. The following parameters were extracted from the computed line profile; resonance energy (zero field) equals 47 997.49 cm^{-1}, polarization equals 55%, Doppler line width equals 0.644, asymmetry parameter equals 43%, apparatus resolution equals 0.55, the product of the magnetic field and the g value equals 5.7, and Nfl equals 2.009. In order to match the observed and calculated profiles, an offset equals 23 619,

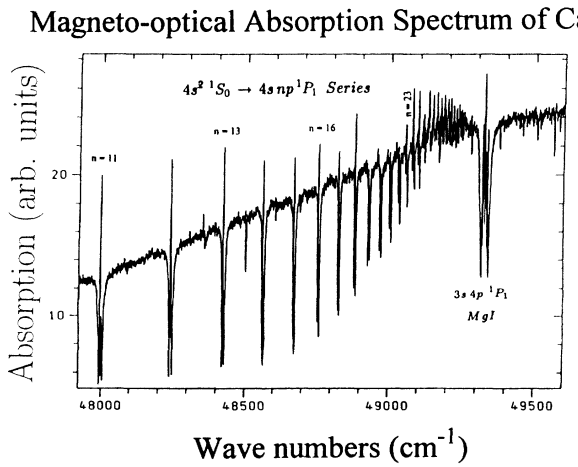

FIG. 1. Magneto-optical rotation absorption spectrum of the principal series ($4snp\ ^1P_1$) of calcium in the spectral region between 2020–2090 Å. Above the ionization threshold, the magneto-optical rotation pattern is due to the $3s4p\ ^1P_1$ transition of magnesium, which was present as an impurity in the calcium sample.

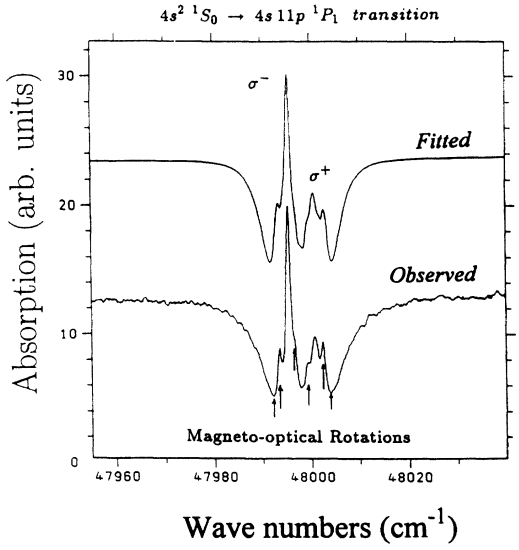

FIG. 2. Calculated and experimental magneto-optical rotation patterns for the $4s11p\ ^1P_1$ line in calcium with magnetic field at 5.7 T. The extracted parameters are as follows: resonance energy equals 47 997.49 cm^{-1}, polarization equals 55%, Doppler line width equals 0.644, asymmetry parameter equals 43%, instrumental resolution equals 0.55, product of the magnetic field and the g factor equals 5.7, and Nfl equals 2.009.

slope equals -0.12, and the multiplication factor of -7737.97 were incorporated in the fitting subroutine.

With a similar fitting procedure we have determined the product Nfl for all the observed line profiles with $11 \leq n \leq 25$. As the number density N and the length of the absorption column l remains constant for a single exposure spectrum, the relative f values can, therefore, be determined quite reliably. The derived oscillator strengths are accurate to about 10% on the relative scale. The results are placed on an absolute scale in which the oscillator strength of the $4s11p\ ^1P_1$ line is fixed at $\log_{10}(gf) = -2.69 \pm 0.05$ (Parkinson, Reeves, and Tomkins [11]), where (gf) is the product of the oscillator strength and the statistical weight, which is equal to unity for the ground level. The uncertainties of the $\log_{10}(gf)$ are expressed in logarithms. A comparison between previously known f values and the present measurements are presented in Table I. The columns 1, 2, and 3 represent the principal quantum numbers, energies of the upper levels and effective quantum numbers for each transition, respectively. An inspection of Tables I shows that the experimental error in the absolute f values varies from 12% for the 11p, 17% for the 17p, and increases to about 30% for $n \geq 17$ members of the series. This fact may be attributed to the limited rotations observed in the far wings of the absorption profiles. In addition, the oscillator strengths of a unperturbed Rydberg series decrease with the principal quantum number as $1/(n^*)^3$, which further reduces the possibility of the observation of rotations for high Rydberg members. The relatively higher error in the f values may also be due to the limited resolution and dispersion of our spectrograph.

The photoionization cross section at the ionization

TABLE I. Absolute oscillator strength measurements of the principal series of calcium. $4s^2\,{}^1S_0 \rightarrow 4snp\,{}^1P_1$ ($11 \leq n \leq 25$). The effective quantum number and the resonance energies (in cm^{-1}) are from Brown, Tilford, and Ginter [31].

n	Energy	n^*	Nfl	$\log_{10}(gf)$	$\log_{10}(gf)^a$	$\log_{10}(gf)^b$	$\log_{10}(gf)^c$
7	45 425.39	5.318			−1.49±0.06	−1.48±0.4	−1.71
8	46 479.96	6.231			−1.91±0.06	−1.90±0.04	−2.20
9	47 184.43	7.192			−2.26±0.05	−2.25±0.04	−2.58
10	47 662.10	8.170			−2.49±0.05	−2.52±0.04	−2.91
11	47 997.49	9.158	2.009	−2.69±0.05	−2.69±0.05	−2.75±0.04	−3.12
12	48 240.53	10.149	1.201	−2.91±0.05	−2.86±0.05	−2.94±0.04	−3.31
13	48 422.09	11.142	0.797	−3.09±0.05	−3.06±0.06	−3.11±0.04	−3.29
14	48 561.10	12.138	0.578	−3.23±0.05	−3.16±0.08	−3.25±0.04	−3.61
15	48 669.83	13.134	0.427	−3.36±0.06	−3.26±0.08	−3.34±0.04	−3.74
16	48 756.45	14.131	0.326	−3.48±0.06	−3.36±0.08	−3.43±0.4	−3.85
17	48 826.54	15.129	0.243	−3.61±0.07		−3.55±0.4	−3.96
18	48 884.06	16.127	0.185	−3.73±0.08			−4.05
19	48 931.82	17.126	0.137	−3.86±0.09			−4.06
20	48 971.93	18.124	0.102	−3.98±0.10			−4.18
21	49 005.92	19.124	0.085	−4.06±0.12			
22	49 034.98	20.123	0.067	−4.17±0.12			
23	49 060.02	21.122	0.065	−4.18±0.13			
24	49 081.75	22.122	0.055	−4.25±0.014			
25	49 100.72	23.121	0.036	−4.44±0.015			

[a]Parkinson, Reeves, and Tomkins [11], oscillator strengths measured by the hook method.
[b]Shabanova [9], oscillator strengths measured by the hook method.
[c]Anderson, Zilitis, and Sarakina [40], oscillator strength calculated semiempirically.

threshold is determined by extrapolating the oscillator strength density to the threshold since (Friedrich [33]),

$$\lim_{n\to\infty} f_n\{dE_n/dn\}^{-1} = df/dE|_{E-E_0}\ , \tag{15}$$

where f_n is the oscillator strength of the $4s^2\,{}^1S_0 \rightarrow 4snp\,{}^1P_1$ transition, E_n is the resonance energy, and E_0 is the ionization threshold energy. The effective quantum number (n^*) is related to the ionization energy by the expression

$$E_n = E_0 - R/(n^*)^2\ , \tag{16}$$

where R is the mass corrected Rydberg constant for calcium 109 736.76 cm^{-1} and $n^* = (n-\mu)$, where μ is the quantum defect. At high n value, the energy separation becomes

$$dE_n/dn = 2R/(n^*)^3\ . \tag{17}$$

The total cross section at the threshold is related to df/dE by

$$\sigma(E) = 4\pi^2\alpha(\hbar/2m_e)df/dE \tag{18}$$

or numerically

$$\sigma(Mb) = 8.85\times10^5\ df/dE(\text{cm})\ ,$$

where α is the fine structure constant and m_e is the electron mass.

The left-hand side of Eq. (15) represents the oscillator strength of a Rydberg state divided by the energy spacing of the transitions at E_n and E_{n+1}. In Fig. 3, we have plotted histograms, which represent the f value of each discrete level as the area of the rectangular block of width $2R/(n^*)^3$ and height $f_n(n^*)^3/2R$ centered at the corresponding transition energy. A smooth extrapolation curve through the differential oscillator strength (df/dE) plot yields the value of the absorption cross section at the

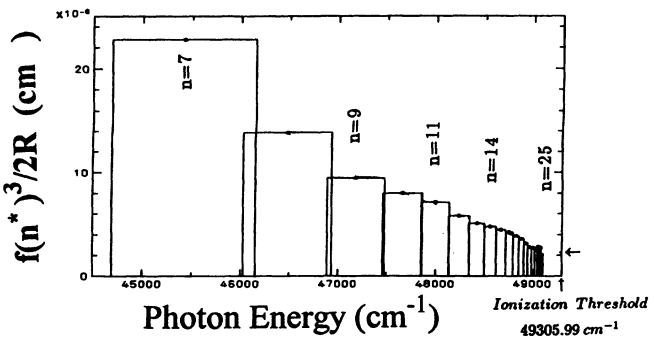

FIG. 3. Differential oscillator strength distribution (df/dE) in the discrete spectrum of calcium from $4s7p\,{}^1P_1$ to $4s25p\,{}^1P_1$. For the sake of completeness, we have included oscillator strengths for the $4s7p\,{}^1P_1$ to $4s10p\,{}^1P_1$ lines form Parkinson, Reeves, and Tomkins [11]. The oscillator strength density at the threshold is determined by a smooth linear extrapolation through the df/dE plot ($7 \leq n \leq 25$), marked as an arrow, as $(2.3\pm0.2)\times10^{-6}$ (cm) or $\sigma = 2.04$ Mb in cross-section units.

ionization threshold. The interpolated oscillator strength density at threshold is $(2.30\pm0.20)\times10^{-6}$ (cm), which is equal to 2.04 Mb, in units of cross section. This value is not far from that extrapolated value by Parkinson, Reeves, and Tomkins [11], which is equal to 2.76 Mb, from experimental measurements ($4\leq n\leq16$). Geiger [34], using the multichannel quantum-defect theory calculated the oscillator strength density at the threshold as 2.07×10^{-6} (cm), which is in excellent agreement with the present value. Scott, Kingston, and Hibbert [36] using the R-matrix method calculated the photoionization cross section at the $4s(^2S_{1/2})$ threshold as 3.5 Mb. Altun, Carter, and Kelly [37], using the many-body perturbation theory and including the double electron resonances, reported the photoionization cross section as 1.0 Mb (length) and 1.5 Mb (velocity). The relativistic random phase approximation calculations [38] yield the threshold cross section value as 2.0 Mb, which is in excellent agreement with the present experimental value.

It is worth noting that the differential oscillator strength (df/dE) curve of the principal series of CaI shows a smooth linear behavior up to $n=18$, at which point there is a sharp drop. Since the Rydberg series reveals a constant quantum defect the possibility of perturbation due to an intruder which could cause the reduction in the oscillator strength, can be ruled out. Alternatively, the emergence of the intercombination series could also borrow the oscillator strength from the adjacent singlet series but we have not detected these lines. A likely explanation for this departure from the linear behavior at high n values has recently been given by Nawaz, Farooq, and Connerade [39]. The high magnetic field leads to the emergence of the satellites due to l mixing necessarily causing a reduction in the oscillator strength of the main transition. Although in the present work we have not been able to observe clearly the residual satellite structure, the effects of magnetic fields are well documented (Garton, Tomkins, and Crosswhite [41,42]).

V. CONCLUSION

We have measured the relative oscillator strengths of the principal series of calcium from $n=11-25$. The derived oscillator strengths are believed to be accurate to about 10% on a relative sale. We have placed the oscillator strengths on an absolute scale by reference to the data for the $4s11p\ ^1P$ line, and this absolute scale is correct to within ±0.06 or 15%. The photoionization cross section at threshold is determined by extrapolation of the density of oscillator strengths, using quantum-defect method, and is found to be in good agreement with the previous experimental and theoretical value.

ACKNOWLEDGMENTS

It is a pleasure to acknowledge many fruitful discussions on the analysis of the experimental data with Professor J. P. Connerade at Imperial College, London, and Professor T. F. Gallagher at the University of Virginia. Technical support received from Dr. Greismann, Dussa, and Kaenders at the Physikalisches Institute der Universitat Bonn during the experimental work is highly appreciated. One of us (I.A.) is thankful to DAAD (German Academic Exchange Service, Germany) and to Quaid-i-Azam University Islamabad for financial support. Financial support from the Alexander von Humboldt Stiftung to M.A.B. is gratefully acknowledged.

[1] A. C. G. Mitchell and M. W. Zemansky, *Resonance Radiation and Excited Atoms* (Cambridge University Press, Cambridge, 1971).
[2] M. C. E. Huber and R. J. Sandeman, Rep. Prog. Phys. **49**, 397 (1986).
[3] W. Gawlik, J. Kawalski, R. Neuman, H. Wiegemann, and K. J. Winkler, J. Phys. B **12**, 3873 (1979).
[4] W. R. S. Garton, J. P. Connerade, M. A. Baig, H. Hormes, and B. Alexa, J. Phys. B **16**, 389 (1983).
[5] B. Alexa, M. A. Baig, J. P. Connerade, W. R. S. Garton, J. Hormes, and T. A. Stavrakas, Nucl. Instrum. Methods **208**, 841 (1983).
[6] J. P. Connerade, H. Ma, N. Shen, and T. A. Stavrakas, J. Phys. B **21**, L241 (1988).
[7] J. P. Connerade, W. A. Farooq, H. Ma, M. Nawaz, and N. Shen, J. Phys. B **25**, 1405 (1992).
[8] Y. I. Ostrovskii and N. Y. Penkin, Opt. Spektrosk. **10**, 429 (1961) (USSR) [Opt. Spectros. **10**, 219 (1961)].
[9] L. N. Shabanova, Opt. Spektrosk. **15**, 829 (1963) [Opt. Spectros. (USSR) **15**, 450 (1963)].
[10] W. H. Smith and H. S. Liszt, J. Opt. Soc. Am. **61**, 938 (1971).
[11] W. H. Parkinson, E. M. Reeves, and F. S. Tomkins, J. Phys. B **9**, 157 (1976).
[12] G. Smith and D. St. Raggett, J. Phys. B **14**, 4015 (1981).
[13] J. J. Wynne and R. Beigang, Phys. Rev. A **23**, 2736 (1981).
[14] K. Ueda, Y. Hamaguchi, and K. Fukuda, Jpn. J. Phys. **48**, 345 (1982).
[15] R. W. Ditchburn and R. D. Hudson, Proc. R. Soc. London Ser. A **256**, 53 (1960).
[16] G. H. Newsom, Proc. Phys. Soc. London **87**, 975 (1966).
[17] V. L. Carter, R. D. Hudson, and E. L. Breig, Phys. Rev. A **4**, 821 (1971).
[18] T. J. McIlrath and R. J. Sandeman, J. Phys. B **5**, 2217 (1972).
[19] N. Karamatskos, M. Muller, M. Schmidt, and P. Zimmermann, J. Phys. B **18**, L107 (1985).
[20] U. Griesmann, N. Shen, J. P. Connerade, K. Sommer, and J. Hormes, J. Phys. B **21**, L83 (1988).
[21] C. Hoeffner, Diplomarbeit, University of Bonn Report No. Bonn-IR-87-40, 1987 (unpublished).
[22] P. Dresbach, Diplomarbeit, University of Bonn, Report No. Bonn-IR-89-28, 1989 (unpublished).
[23] W. Dussa, Ph.D. thesis, University of Bonn Report No. Bonn-IR-92, 1992 (unpublished).
[24] M. A. Baig and J. P. Connerade, J. Phys. B **17**, 1101 (1984).
[25] M. A. Baig, S. Ahmad, J. P. Connerade, S. A. Bhatti, and N. Ahmad J. Phys. B **25**, 321 (1992).
[26] V. Kaufman, and B. Edlen, J. Phys. Chem. Ref. Data **3**, 825 (1974).
[27] J. P. Connerade, J. Phys. B **16**, 399 (1983).

[28] J. P. Connerade, T. A. Stavrakas, and M. A. Baig in *Synchrotron Radiation Sources and Their Applications,* Proceedings of the Thirtieth Scottish Universities Summer School in Physics, 1985, edited by G. N. Greaves and I. H. Munro (Aberdeen University Press, Aberdeen, 1989).
[29] W. R. S. Garton and K. Codling, Proc. Phys. Soc. London **86**, 1067 (1965).
[30] N. P. Penkin and L. N. Shabanova, Opt. Spektrosk. **18**, 941 (1965) [Opt. Spectrosc. (USSR) **18**, 535 (1965)].
[31] C. M. Brown, S. C. Tilford, and M. L. Ginter, J. Opt. Soc. Am. **63**, 1454 (1973).
[32] J. A. Armstrong, J. J. Wynne, and P. Esherick, J. Opt. Soc. Am. **69**, 211 (1979).
[33] H. Friedrich, *Theoretical Atomic Physics* (Springer, Berlin, 1991).
[34] J. Geiger, J. Phys. B **12**, 2277 (1979).
[35] C. Barrientos and I. Martin Can. J. Phys. **66**, 29 (1988).
[36] P. Scott, A. E. Kingston, and A. Hibbert, J. Phys. B **16**, 3945 (1983).
[37] Z. Altun, S. L. Carter, and H. P. Kelly, Phys. Rev. A **27**, 1943 (1983).
[38] P. C. Deshmukh and W. R. Johnson, Phys. Rev. A **27**, 320 (1983).
[39] M. Nawaz, W. A. Farooq, and J. P. Connerade, J. Phys. B **25**, 5327 (1992).
[40] E. M. Anderson, V. A. Zilitis, and E. S. Sarakina, Opt. Spektrosk. **23**, 513 (1967) [Opt. Spectrosc. (USSR) **23**, 279 (1967)].
[41] W. R. S. Garton and F. S. Tomkins, Astrophys. J. **158**, 839 (1969).
[42] W. R. S. Garton, F. S. Tomkins, and H. M. Crosswhite, Proc. R. Soc. London, Ser. A **373**, 189 (1980).